

Property improvement of $0.3\text{Pb}(\text{Zn}_{1/3}\text{Nb}_{2/3})\text{O}_3$ - $0.7\text{Pb}_{0.96}\text{La}_{0.04}(\text{Zr}_x\text{Ti}_{1-x})_{0.99}\text{O}_3$ ceramics by hot-pressing

Guochu Deng, Aili Ding*, Xinsen Zheng, Xia Zeng, Qingrui Yin

State Key Laboratory of High Performance Ceramics and Superfine Microstructure, Shanghai Institute of Ceramics,
Chinese Academy of Sciences, 1295 Dingxi Road, Shanghai 200050, PR China

Received 10 January 2005; received in revised form 27 March 2005; accepted 9 April 2005

Available online 13 May 2005

Abstract

The piezoelectric ceramics of the compositions expressed by the formula: $0.3\text{Pb}(\text{Zn}_{1/3}\text{Nb}_{2/3})\text{O}_3$ - $0.7\text{Pb}_{0.96}\text{La}_{0.04}(\text{Zr}_x\text{Ti}_{1-x})_{0.99}\text{O}_3$ ($x = 0.50$ – 0.53) were prepared by two kind of sintering processes: conventional sintering (CS) and hot-pressing (HP) sintering. By comparing the properties of these two series of ceramics, piezoelectric coefficients (d_{33}), electromechanical coupling factors (k_p), dielectric constants (ϵ_r), etc. were enormously improved by HP sinter procedure, which can be attributed to the highly dense microstructure (bulk density >99%). The most impressive results are the d_{33} (845 pC/N) and k_p (0.703) in the HP specimen with Zr/Ti = 51/49, which have not been observed in the previous relative reports. Additionally, according to the contrast of the experiment data, the origin of the property improvement was analyzed in details. © 2005 Elsevier Ltd. All rights reserved.

Keywords: Hot-pressing; Piezoelectric properties; Dielectric properties; Grain boundaries; $\text{Pb}(\text{Zn},\text{Nb})\text{O}_3$; PLZT

1. Introduction

In recent years, there has been an increasing demand for high performance piezoelectric materials.^{1–3} Many relaxor-ferroelectric based piezoelectric solid solutions systems have been developed to satisfy this demand.^{4,5} Intensive studies were conducted to obtain single crystals of the typical relaxors, such as $\text{Pb}(\text{Zn}_{1/3}\text{Nb}_{2/3})\text{O}_3$ - PbTiO_3 (PZN-PT)⁶ and $\text{Pb}(\text{Mg}_{1/3}\text{Nb}_{2/3})\text{O}_3$ - PbTiO_3 (PMN-PT),⁷ due to the discovery of their substantial piezoactivity and electromechanical properties. However, compositional uniformity throughout the crystal is difficult to achieve using conventional solution growth method with PbO fluxes.⁸

Great efforts have also been taken to prepare ceramics of these systems near the morphotropic phase boundary (MPB). It is difficult to synthesize pure perovskite ceramics because competitively grown pyrochlore phase seems unavoidable.^{9,10} Though Swartz et al.¹¹ had succeeded in

synthesizing the PMN-PT ceramics with pure perovskite phase near MPB by a two-stage columbite method, PZN-PT ceramics at MPB were not obtained by this method because of the formation of pyrochlore. The addition of other perovskite materials, such as lead titanate (PbTiO_3), barium titanate (BaTiO_3), and $\text{Pb}(\text{Ti},\text{Zr})\text{O}_3$ (PZT)¹² has been found to be effective in stabilizing PZN in the perovskite structure. In the past researches, some fine piezoelectric properties ($d_{33} = 430$ pC/N, $k_p = 0.67$) were observed in the PZT-modified PZN ceramics near the MPB compositions.^{13,14}

PZN-PZT ceramics were considered to be sintered into ceramics at a relative low temperature, so it was very difficult to achieve the full density.^{15,16} Because of fast growth, liquid phase and non-diffusible gas such as N_2 , there were a large amount of pores trapped in the ceramic matrix during sintering process.^{8,17} High porosity is an impediment to property improvement of the ceramic products. Therefore, densification of this kind of ceramics will be an effective way to enhance their performance.

Hot uniaxial pressing has been developed for the production of high quality transparent ceramics such as $(\text{Pb},\text{La})(\text{Zr},\text{Ti})\text{O}_3$ (PLZT).¹⁸ At the same time, it can be used to

* Corresponding author. Tel.: +86 21 52412364; fax: +86 21 52413122.

E-mail addresses: goldtruth@mail.sic.ac.cn (G. Deng),
alding@mail.sic.ac.cn (A. Ding).

intensively raise the bulk density of ceramics. Oxygen atmosphere is also helpful to increase the mobility of oxygen vacancies and dispel the non-diffusible pores. In this study, the hot-pressing procedure was introduced into preparation of $0.3\text{Pb}(\text{Zn}_{1/3}\text{Nb}_{2/3})\text{O}_3$ - $0.7(\text{Pb},\text{La})(\text{Zr},\text{Ti})\text{O}_3$ (PZN-PLZT) piezoceramics. So the effect of hot-pressing on the performance of PZN-PLZT was investigated by comparing with conventional sintered specimens.

2. Experimental procedure

Compositions were selected according to the following formula:



where $x = 0.50$ – 0.53 . $0.3\text{Pb}(\text{Zn}_{1/3}\text{Nb}_{2/3})\text{O}_3$ - $0.7(\text{Pb},\text{La})(\text{Zr},\text{Ti})\text{O}_3$ (PZN-PLZT) ceramic specimens were prepared by two sintering procedures: conventional sintering (CS) and hot-pressing (HP).

For the CS and HP procedures, ceramic powders of PZN-PLZT were synthesized using the columbite precursor method.¹¹ In this two-step process, the ZnNb_2O_6 was formed from ZnO (99.9%) and Nb_2O_5 (99.99%). Stoichiometric amounts of ZnO and Nb_2O_5 were mixed and milled in ethanol for 4 h. After drying, the mixture was calcined at 1000°C for 2 h in a closed alumina crucible. The obtained ZnNb_2O_6 precursor was then mixed with other metal oxides (PbO , TiO_2 , ZrO_2) in a stoichiometric ratio (for the HP specimens, 10% excess PbO) to form the desired compositions. The excess PbO was used in order to form a liquid in the specimens to promote densification during the sintering process. The mixture was calcined at 800°C for 2 h in air, remilled, pressed into disks in different diameters ($\varnothing 12$ mm and $\varnothing 25$ mm) for CS and HP processes, respectively. During the CS process, the specimens were packed in a double-crucible set-up using PbTiO_3 as the packing powder to control PbO volatilization, and sintered at 1250°C for 2 h. In the HP process, the specimens were sintered at 1200°C for 3 h under a uniaxial pressure of 160 MPa and O_2 gas flow of $5\text{ cm}^3/\text{min}$, and then soaked at 1150°C for 10 h without pressure.

The phase structures of obtained products were characterized by XRD, and their microstructures were analyzed by SEM. The XRD patterns indicated the specimens contained a homogeneous monophase: perovskite (to the extent of XRD resolution). The transition from rhombohedral to tetragonal phase was also detected with the increase of PZ content for the HP specimens, which confirm the composition was cross the MPB of this complex ceramic system. The transition was not observed in the CS specimens. The bulk densities of CS and HP specimens were measured by Archimedes method.

Before electric measurements, all sintered specimens were polished and gold electrodes were sputtered on the large surfaces. And then, they were poled in air at 210°C by applying an electric field of $10\text{ kV}/\text{cm}$ for 15 min, followed by cooling under the same electric field.

For resonance measurements, specimen dimensions were in accordance with the IEEE standards for resonance measurements. The dielectric constant was measured at room temperature on an impedance analyzer (Agilent 4294A Precision Impedance Analyzer, Melrose, USA). Poled and unpoled maximum dielectric constants are obtained from dielectric spectrum measured during heating and cooling processes, respectively. The piezoelectric coefficients (d_{33}) of the CS and HP specimens were measured by a quasi-static piezoelectric d_{33} -meter (ZJ-3A, Institute of Acoustics Academic Sinica, Beijing, China), and the electromechanical coupling factor (k_p) was determined by the same impedance analyzer with the resonance and antiresonance technique, according to the following relationship:^{15,19}

$$k_p = \left(\frac{(f_a - f_r)}{[0.395f_r + 0.574(f_a - f_r)]} \right)^{1/2}$$

Where f_r and f_a are the resonance and antiresonance frequencies, respectively.

3. Results and discussions

3.1. Microstructure

The XRD patterns of 0.3PZN - 0.7PLZT ($\text{Zr}/\text{Ti} = 50/50$ to $53/47$) obtained by the CS and HP process are shown in Fig. 1(a) and (b), respectively. As can be seen, all of the patterns for the CS and HP specimens exhibit the characteristics of pure perovskite phase. Several patterns for the specimens with high Zr/Ti ratio display weak peaks of secondary phase, which can be identified as the $\{222\}$ peak of pyrochlore phase. Since PbTiO_3 (PT) is more effective than PbZrO_3 (PZ) to stabilize the perovskite phase of PZN, PZN-PLZT becomes more and more unstable with the increasing of PZ contents. The mainly differences of these XRD patterns are focused on the peaks of $\{200\}$ reflection near 45° because the $\{200\}$ reflection results in a single peak for the rhombohedral phase, whereas it splits into two peaks for the tetragonal phase.²⁰ All of the patterns in Fig. 1(a) show split peaks around 45° , and these split peaks became more and more evident with the decrease of Zr/Ti ratio. Such result indicates that the obtained CS specimens possess tetragonal structure. From the trend of the patterns of the HP specimens (Fig. 1(b)), it is indicated that the microstructures of these complex compounds experience a gradual transition process from tetragonal to rhombohedral phase with the increase of Zr/Ti ratio. According to certain previous reports,^{15,19,20} the MPB can be defined as the co-existence of tetragonal and rhombohedral phases. Therefore, the MPB of 0.3PZN - 0.7PLZT ($\text{La} = 4\text{ mol}\%$) complex system can be delimited in the range of $\text{Zr}/\text{Ti} = 51/49$ to $52/48$ ratio.

Fig. 2(a) is the SEM image of the fractured surface of a typical CS specimen. From this image, the grain boundary cannot be identified, and the fractured surface shows the features of

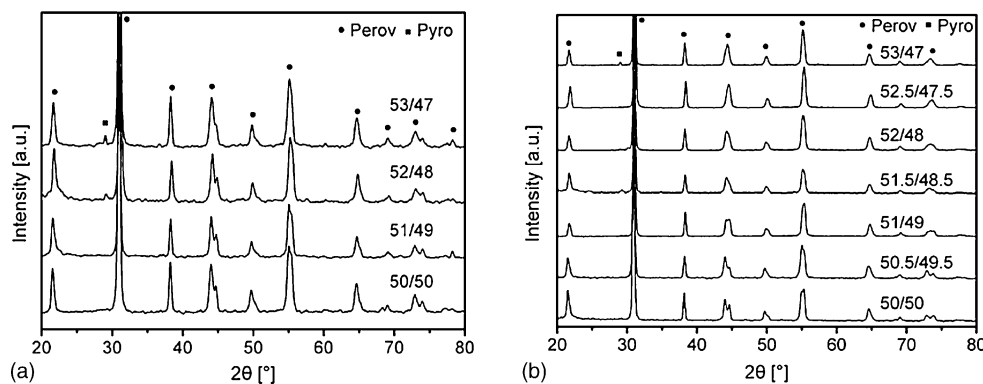


Fig. 1. XRD patterns of the CS (a) and HP (b) specimens with various Zr/Ti ratios.

typical transgranular fractures. Since there is an obvious pore in the image area, the grain size in the CS specimen can be identified as 5–6 μm . Comparing with the fractured surface of the CS specimen, the fractured surface of the HP specimen (Fig. 2(b)) displays the characteristics of intergranular fracture with smaller grain size about 2–3 μm , and high density without obvious pores.

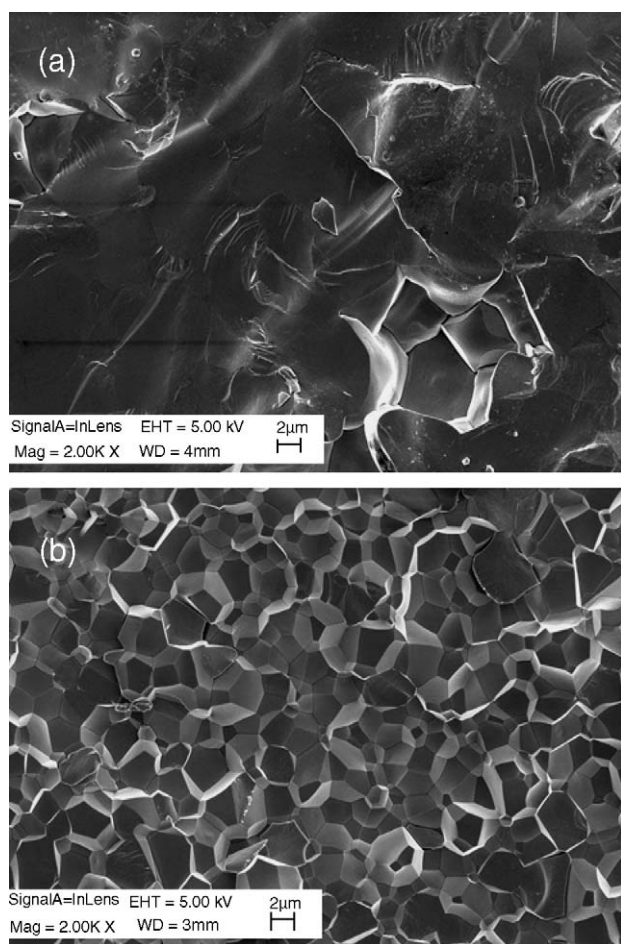


Fig. 2. SEM micrographs of the fractured surfaces of the CS (a) and HP (b) specimens with Zr/Ti = 51/49.

Bulk density of piezoceramics is an important factor influencing the properties of ceramics. Commonly, the dielectric and piezoelectric properties are positively correlated with the density of the specimens.^{21,22} The bulk densities of the CS and HP specimens are plotted in Fig. 3. We can see that the densities of all HP specimens are quite close to the theoretical density (>99% of the theoretical density values, which were calculated according to XRD data), and much higher than those of the CS specimens. These results are consistent with the SEM images.

3.2. Comparison of properties

Piezoelectric coefficient (d_{33}) is one of the most important parameters to characterize the piezoactivity of ceramic specimens, which are a key property for applications, such as actuators and transducers. The piezoelectric coefficients of the CS and HP PZN-PLZT specimens with various Zr/Ti ratios are shown in Fig. 4. The coefficients of the HP specimens are greatly influenced by the Zr/Ti ratio in the PZT: The variations are greater than 40% when the Zr/Ti ratio shifts only 2%. The HP curve in Fig. 4 shows a trend of increasing and then decreasing, and achieves the maximum (845pC/N)

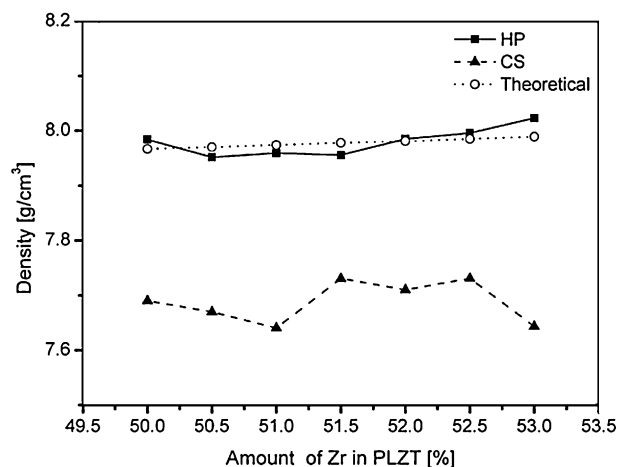


Fig. 3. Bulk densities of the CS and HP PZN-PLZT specimens with various Zr amounts.

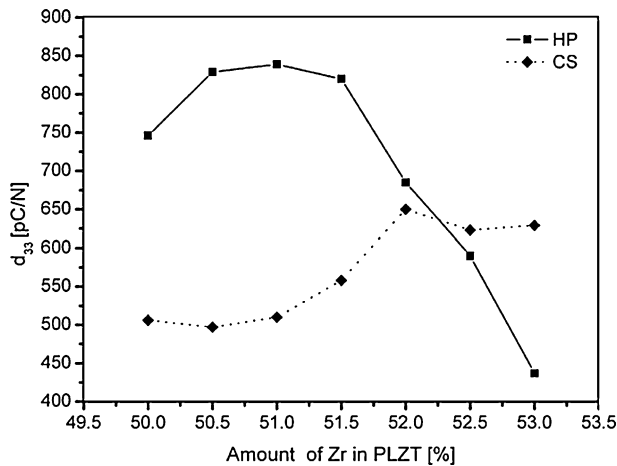


Fig. 4. Piezoelectric coefficients of the CS and HP PZN-PLZT specimens with various Zr amounts.

at the $Zr/Ti = 51/49$. This kind of high d_{33} value has not been observed in the PZN-PZT ceramic systems previously reported.^{14,19} The CS curve displays a similar trend with a small variation, but the maximum of d_{33} value (637 pC/N) shifts to the $Zr/Ti = 52/48$. Generally, the HP specimens have higher piezoactivity than the CS specimens.

Electromechanical coupling factor is another critical property of piezoceramics for applications in transducers. Fig. 5 plots the changing tendencies of the planar coupling factors (k_p) of the HP and CS specimens with different Zr/Ti ratio. Similar to the values of d_{33} , the k_p values of the HP specimens form a parabola shape, and reach the peak value (0.703) at the same Zr/Ti ratio of 51/49. According to the previous references,^{23,24} this kind of high k_p values have been obtained in a few complex systems such as $Pb(Sc_{1/2}Nb_{1/2})O_3$ - $PbTiO_3$ (PSN-PT).²³ However, PZN-PLZT is a cost-advantageous alternative for high k_p values since Sc is an extremely expensive rare earth element. The k_p values of CS specimens also such exhibit a similar trend with increasing Zr/Ti ratio, whereas the maximum (0.59) of the k_p values shift to the higher PZ content.

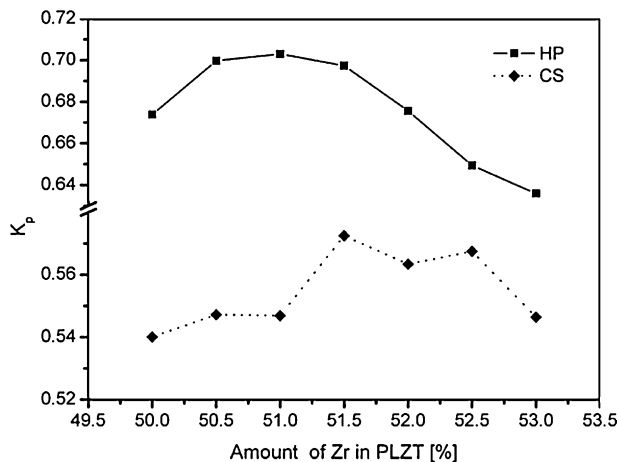


Fig. 5. k_p of the CS and HP PZN-PLZT specimens with various Zr amounts.

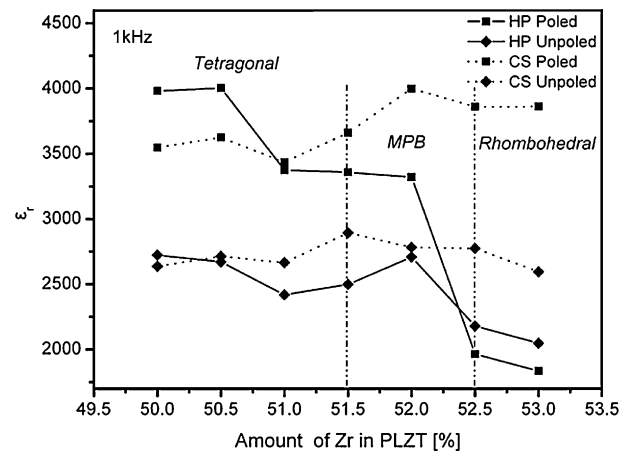


Fig. 6. Dielectric constants of the CS and HP PZN-PLZT specimens at room temperature with various Zr amounts; The MPB region is for the HP specimens.

In Fig. 6, the dielectric constant of the HP and CS specimens at room temperature shows a very complex trend. For the HP specimens, the dielectric constants of poled specimens are larger than those of the unpoled specimens at the tetragonal side. The results are averse at the rhombohedral side. For the CS specimens, all dielectric constants of poled specimens are larger than those of unpoled specimens. The poled and unpoled dielectric constants of the HP specimens are not higher than those values of the CS specimens, which is different from the above d_{33} and k_p results and would be discussed in latter part.

The temperature (T_m) of dielectric maximum (Fig. 7) indicates that the T_m decrease with the increase of the Zr/Ti ratio. This trend is easy to understand since that $PbTiO_3$ possesses a higher Curie temperature (490 °C) than $PbZrO_3$ (230 °C). And the T_m of HP specimens are higher than those of CS specimens.

Fig. 8(a) and (b) plot the hysteresis loops of CS specimens and HP specimens, respectively. From these two figures, the

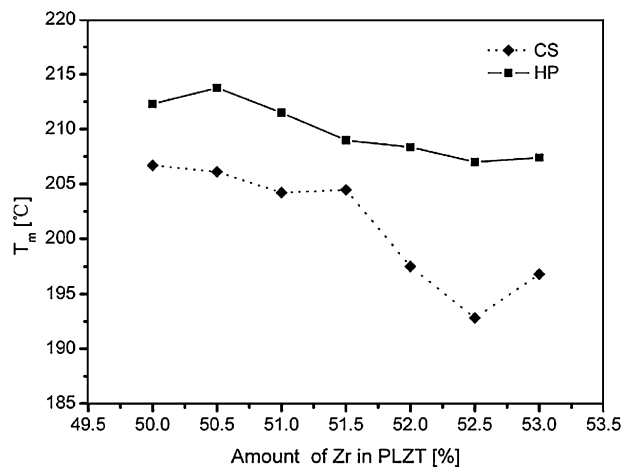


Fig. 7. The temperature of dielectric maximum of the CS and HP PZN-PLZT specimens with various Zr amounts.

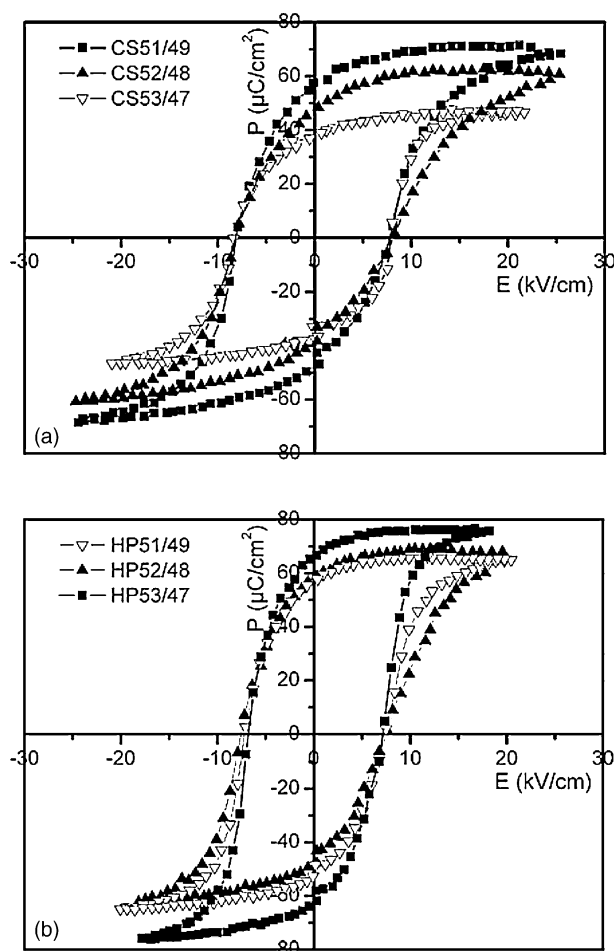


Fig. 8. Hysteresis loops of the CS (a) and HP (b) PZN-PLZT specimens.

remnant polarizations (P_r) of HP and CS show two different trends with the increase of Zr/Ti ratio: decreasing in CS specimens while increasing in HP specimens. The coercive field (E_c) of HP specimens was uniform (about 7.1 kV/cm), but lower than the value (7.5 kV/cm) for CS specimens. Additionally, the shape of the hysteresis loops for HP specimens was closer to a “square loop” than for CS specimens. And the HP specimens more easily reached the saturation polarization than the CS specimens. These results imply that HP specimens were “softer” than CS specimens.

3.3. Discussing of results

The above results show that the HP procedure greatly influenced the properties of the ceramics. Firstly, the property changes are considered one by one.

The d_{33} and k_p values were enormously enhanced by the HP procedure and their maximum values shifted to a lower PZ content. Commonly, the maxima of dielectric coefficient and electromechanical coupling factor appear on the tetragonal side near the MPB.^{25,26} The observed shifts of the maxima of d_{33} and k_p may be attributed to the shift of the MPB and

the densification. This reasoning is supported by the XRD data.

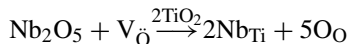
The poled dielectric constants of the HP specimens display a sharp drop from tetragonal to rhombohedral phase even lower than unpoled values, whereas those of the CS specimens are higher than unpoled ones for all compositions (Fig. 6). This result coincides with some previous reports in PNN-PMN-PZT, PZN-PMN-PZT²⁴, PZT²⁷ etc. systems. According to Fesenko et al.²⁷, dielectric constants in tetragonal phase and rhombohedral phase present two different changes relative to microstructure: In the tetragonal phase, polarization will cause the relieving of the clamping effect, which increases the dielectric constant, while in the rhombohedral phase, the reorientation after polarization causes the obvious dielectric anisotropy, which reduces the dielectric constant along polarization direction. Therefore, the dielectric results of the HP and CS specimens imply that the compositions from Zr/Ti = 50/50 to 53/47 run across the MPB for the HP specimens, but are located in the tetragonal region for the CS specimens. Such speculation is consistent with the XRD results in Fig. 1.

By analyzing the results above, it can be found that the properties of the HP specimens, such as high d_{33} , k_p , P_r and low E_c , were optimized by the HP procedure. Obviously, the HP specimens are softer than the CS specimens. Such optimization can be attributed to the following factors. Firstly, the HP procedure removed the pores in the samples and greatly enhanced the specimen density, which is critical to many piezoelectric properties, such as d_{33} , k_p , etc.²¹ Though HP procedure inhibited grain growth, the effect of low porosity is not counteracted by this reduced grain size.

Assuming that such explanation is right, the dielectric constant of HP specimens should much higher than that of porous CS specimens. However, the experimental data from the HP specimens were just slightly higher than those values of the CS specimens. Since the poled and unpoled specimens present nearly the same trend, the domain and stress effect can be ruled out. Therefore, this maybe results from the second effect—grain boundary effect. The scanning electron microscopy observations of fractured surfaces of HP specimens indicated primarily intergranular fractures, which suggest weak grain boundaries and the presence of a different phase (pyrochlore) located in the grain boundaries.¹¹ The phase boundary usually belongs to amorphous phase with a low dielectric constant. As the grain size is smaller, the number of boundaries in series with the grains increases. So the dielectric constants of the HP specimens were affected by these large grain boundary volumes. Thus, the dielectric constants of the HP specimens are slightly higher than those of CS ones.

Composition is the third factor influencing the property differences between the two series of specimens. The long sintering time during the HP procedure will cause volatilization of PbO.¹¹ and a small amount of Zn. Consequently, the HP specimens present the characteristics of specimen doped by Nb^{5+} . According to the previous references, Nb_2O_5 is a

good donor dopant for PZT-based ceramics, which will increase the mobility of the domain walls.²⁸ The defect chemistry reaction is supposed to take place via the following equations, which reduce the concentration of oxygen vacancy, which is the main factor for pinning the mobility of domain walls.²⁹



High values of piezoelectric coefficient d_{33} and electromechanical coupling coefficient k_p in poled PZT-based ceramics are believed to arise from the motion of domain walls under the action of applied field or stress.^{30–32} Additionally, a small amount of doping Nb^{5+} will increase the densification and reduce the grain sizes of ceramics during the sintering procedure.^{30–32} These phenomena can all be observed in our results. Certainly, the increase of bulk density and small grain size is mainly attributed to the hot-pressing procedure under oxygen atmosphere because the application of pressure during sintering process helps to expel pores and to suppress grain growth.

4. Conclusion

The ceramic specimens of PZN-PLZT system were prepared by the CS and HP procedure. The HP sintering procedure greatly improves the densities of PZN-PLZT ceramic specimens. With the densification of the HP specimens, the piezoelectric and dielectric properties, such as d_{33} , k_p , P_r , etc. were enhanced to a great extent. Especially, the optimum piezoelectric coefficient (845 pC/N) and planar coupling factor (0.703) were obtained in the HP specimens. At the same time, the effect of the HP procedure on the material properties was analysed; the material density is one of the most important factors influencing their properties.

Acknowledgements

This project is financially supported by the National ‘863’ (2002AA325080) and ‘973’ (2002CB6133055) programs of China.

References

- Uchino, K., Electrostrictive actuators: materials and applications. *Am. Ceram. Soc. Bull.*, 1986, **65**, 647–651.
- Park, S. E. and Shrout, T. R., Characteristics of relaxor-based piezoelectric single crystals for ultrasonic transducers. *IEEE Trans. Ultrason. Ferroelectr. Freq. Control*, 1997, **44**, 1140–1147.
- Park, S. E. and Shrout, T. R., Ultrahigh strain and piezoelectric behavior in relaxor-based ferroelectric single crystals. *J. Appl. Phys.*, 1997, **82**, 1804–1811.
- Shrout, T. R. and Halliyal, A., Preparation of lead-based ferroelectric relaxors for capacitors. *Am. Ceram. Soc. Bull.*, 1987, **66**, 704–711.
- Shrout, T. R., Chang, Z. P. and Lin, I. N., Dielectric behavior of single crystals near the $(1-x)\text{Pb}(\text{Mg}_{1/3}\text{Nb}_{2/3})\text{O}_3$ - $x\text{PbTiO}_3$ morphotropic phase boundary. *Ferroelectr. Lett.*, 1990, **12**, 63–69.
- Dabkowski, A., Dabkowska, H. A., Greedan, J. E., Ren, W. and Mukherjee, B. K., Growth and properties of single crystals of relaxor PZN-PT materials obtained from high-temperature solution. *J. Cryst. Growth*, 2004, **265**, 204–213.
- Zhao, X., Fang, B., Cao, H., Guo, Y. and Luo, H., Dielectric and piezoelectric performance of PMN-PT single crystals with compositions around the MPB: influence of composition, poling field and crystal orientation. *Mater. Sci. Eng. B*, 2002, **96**, 254–262.
- Chung, U.-J., Park, J.-K., Hwang, N.-M., Lee, H.-Y. and Kim, D.-Y., Effect of grain coalescence on the abnormal grain growth of $\text{Pb}(\text{Mg}_{1/3}\text{Nb}_{2/3})\text{O}_3$ -35mol% PbTiO_3 ceramics. *J. Am. Ceram. Soc.*, 2002, **85**, 965–968.
- Gururaja, T. R., Safari, A. and Halliyal, A., Preparation of perovskite PZN-PT ceramic powder near the morphotropic phase boundary. *Am. Ceram. Soc. Bull.*, 1986, **65**, 1601–1603.
- Wakiya, N., Shinozaki, K. and Mizutani, N., Estimation of phase stability in $\text{Pb}(\text{Mg}_{1/3}\text{Nb}_{2/3})\text{O}_3$ and $\text{Pb}(\text{Zn}_{1/3}\text{Nb}_{2/3})\text{O}_3$ using the bond valence approach. *J. Am. Ceram. Soc.*, 1997, **80**, 3217–3220.
- Swartz, S. L., Shrout, T. R., Schulze, W. A. and Cross, L. E., Dielectric properties of lead-magnesium niobate ceramics. *J. Am. Ceram. Soc.*, 1984, **67**, 311–315.
- Halliyal, A., Kumar, U., Newnham, R. E. and Cross, L. E., Stabilization of the perovskite phase and dielectric properties of ceramics in the $\text{Pb}(\text{Zn}_{1/3}\text{Nb}_{2/3})\text{O}_3$ - BaTiO_3 system. *Am. Ceram. Soc. Bull.*, 1987, **66**, 671–676.
- Jiang, X. P., Fang, J. W., Zeng, H. R., Li, G. R., Chen, D. R. and Yin, Q. R., Dielectric properties of $\text{Pb}(\text{Zn}_{1/3}\text{Nb}_{2/3})\text{O}_3$ - PbZrO_3 - PbTiO_3 system in the rhombohedral region near the morphotropic phase boundary. *J. Mater. Res.*, 2000, **15**, 2745–2749.
- Fan, H. and Kim, H. E., Effect of lead content on the structure and electrical properties of $\text{Pb}((\text{Zn}_{1/3}\text{Nb}_{2/3})_{0.5}(\text{Zr}_{0.47}\text{Ti}_{0.53})_{0.5})\text{O}_3$ ceramics. *J. Am. Ceram. Soc.*, 2001, **84**, 636–638.
- Seo, S. B., Lee, S. H., Yoon, C. B., Park, G. T. and Kim, H. E., Low-temperature sintering and piezoelectric properties of $0.6\text{Pb}(\text{Zr}_{0.47}\text{Ti}_{0.53})\text{O}_3$ - $0.4\text{Pb}(\text{Zn}_{1/3}\text{Nb}_{2/3})\text{O}_3$ ceramics. *J. Am. Ceram. Soc.*, 2004, **87**, 1238–1243.
- Hou, Y., Zhu, M., Gao, F., Wang, H., Wang, B., Yan, H. and Tian, C., Effect of MnO_2 addition on the structure and electrical properties of $\text{Pb}(\text{Zn}_{1/3}\text{Nb}_{2/3})_{0.2}(\text{Zr}_{0.5}\text{Ti}_{0.5})_{0.8}\text{O}_3$ ceramics. *J. Am. Ceram. Soc.*, 2004, **87**, 847–850.
- Kim, J.-J., Jun, B.-K., Kim, D.-Y. and Hwang, N. M., Effect of sintering atmosphere on isolated pores during the liquid-phase sintering of MgO - CaMgSiO_4 . *J. Am. Ceram. Soc.*, 1987, **70**, 734–737.
- Haertling, G. H. and Land, C. E., Hot-pressed $(\text{Pb},\text{La})(\text{Zr},\text{Ti})\text{O}_3$ ferroelectric ceramics for electrooptic applications. *J. Am. Ceram. Soc.*, 1971, **54**, 1–11.
- Lee, S. H., Yoon, C. B., Seo, S. B. and Kim, H. E., Effect of lanthanum on the piezoelectric properties of lead zirconate titanate-lead zinc niobate ceramics. *J. Mater. Res.*, 2003, **18**, 1765–1770.
- Fan, H., Park, G. T., Choi, J. J., Ryu, J. and Kim, H. E., Preparation and improvement in the electrical properties of lead-zinc-niobate-based ceramics by thermal treatments. *J. Mater. Res.*, 2002, **17**, 180–185.
- Chu, S.-Y., Chen, T.-Y., Tsai, I.-T. and Water, W., Doping effects of Nb additives on the piezoelectric and dielectric properties of PZT ceramics and its application on SAW device. *Sens. Actuat. A Phys.*, 2004, **113**, 198–203.
- Chu, S.-Y., Doping effects on the dielectric properties of low temperature sintered lead-based ceramics. *Mater. Res. Bull.*, 2000, **35**, 1067–1076.
- Yamashita, Y. J. and Hosono, Y., High dielectric constant and large electromechanical coupling factor relaxor-based piezoelectric ceramics. *Jpn. J. Appl. Phys.*, 2004, **43**, 6679–6682.
- Wang, C. H., Physical and electrical properties of $\text{Pb}_{0.96}\text{Sr}_{0.04}[(\text{Zr}_{0.74}-x\text{Ti}_x)(\text{Mg}_{1/3}\text{Nb}_{2/3})_{0.20}(\text{Zn}_{1/3}\text{Nb}_{2/3})_{0.06}]\text{O}_3$ ceramics near the

- morphotropic phase boundary. *Jpn. J. Appl. Phys.*, 2003, **42**, 4455–4456.
25. Weston, T. B., Webster, A. H. and McNamara, V. M., Variations in properties with composition in lead zirconate-titanate ceramics. *J. Can. Ceram. Soc.*, 1967, **36**, 15–18.
26. Klimov, V. V., Didkovskaya, O. S. and Prisedsky, V. V., Some physico-chemical aspects in development and production of piezoceramic materials. *Ferroelectrics*, 1982, **41**, 97–109.
27. Fesenko, E. G., Dantsiger, A. Y., Resnitoenko, L. A. and Kupriyanov, M. F., Composition-structure-properties dependences in solid solutions on the basis of lead-zirconate-titanate and sodium niobate. *Ferroelectrics*, 1982, **41**, 137–142.
28. Tanasoiu, C., Dimitriu, E. and Miclea, C., Effect of Nb, Li doping on structure and piezoelectric properties of PZT type ceramics. *J. Eur. Ceram. Soc.*, 1999, **19**, 1187–1190.
29. Zou, Q., Ruda, H., Yacobi, B. G. and Farrell, M., Microstructural characterization of donor-doped lead zirconate titanate films prepared by sol–gel processing. *Thin Solid Films*, 2002, **402**, 65–70.
30. Chu, S.-Y., Chen, T.-Y. and Tsai, I.-T., Effects of poling field on the piezoelectric and dielectric properties of Nb additive PZT-based ceramics and their applications on SAW devices. *Mater. Lett.*, 2004, **58**, 752–756.
31. Pereira, M., Peixoto, A. G. and Gomes, M. J. M., Effect of Nb doping on the microstructural and electrical properties of the PZT ceramics. *J. Eur. Ceram. Soc.*, 2001, **21**, 1353–1356.
32. Sakaki, C., Newalkar, B. L., Komarneni, S. and Uchino, K., Grain size dependence of high power piezoelectric characteristics in Nb doped lead zirconate titanate oxide ceramics. *Jpn. J. Appl. Phys.*, 2001, **40**, 6907–6910.